Annexure -III

UNIVERSITY GRANTS COMMISSION

BAHADUR SHAH ZAFAR MARG

NEW DELHI – 110 002.

Annual Report of the work done on the Major Research Project

1	Project report No. 1st/2nd/3rd/Final	Final report
2	UGC Reference No.	F.No. 36-211/2008(SR)
3	Period of report:	From 01/04/2011 to 30/04/2012
4	Title of research project: **"Layer-by-Layer deposition of multicolored conduction polymer composites for electrochromic smart window application"**	
5	(a) Name of the Principal Investigator	Dr. Pramod S. Patil
	(b) Deptt. and University/College where work has progressed	Department of Physics, Shivaji University, Kolhapur-416004
6	Effective date of starting of the project	**01/05/2009**

7 Grant approved and expenditure incurred during the period of the report:

a. Total amount approved Rs. **11,79,000/-**

[Books & Journal: Rs. 20,000/-, Equipment: Rs. 6,00,000/-, Project fellowship 2,88,000/- @ 8,000/- p.m., Chemicals/Glassware: - Rs. 1,00,000/- , Contingency: Rs. 75,000/-, Travel/ Field Work: Rs. 50,000/-, Overhead charges: Rs.46,300/- (Except Travel & Field Work)]

b. Total expenditure

Year	Expenditure
01/05/2009 to 31/03/2010	6,29,842/-
01/04/2010 to 31/03/2011	2,04,352/-
01/04/2011 to 30/04/2012	2,81,823/-
Total	**11,16,017/-**

Total expenditure for [01/04/2011 to 30/04/2012]

[Equipment: Rs. 99,084/-, Project fellowship 96,000/- @ 8,000/- p.m., Chemicals/Glassware: - Rs. 33,276/- , Contingency: Rs. 25,013/-, Travel/ Field Work: Rs. 13,016/-, Overhead charges: Rs. 15,434/-(Except Travel & Field Work)]

Total expenditure for [01/04/2009 to 30/04/2012]

[Books & Journal: Rs. 13709/-, Equipment: Rs. 5,97,360/-, Project fellowship Rs. 263742/- @ 8,000/- p.m., Chemicals/Glassware: - Rs. 94,608/- , Contingency: Rs. 71,706/-, Travel/ Field Work: Rs. 28,592/-, Overhead charges: Rs. 46,300/- (Except Travel & Field Work)]

Report of the Work done

I. Brief objective of the project
See Annexure A

II. Work done so far and results achieved and publications, if any, resulting from the work (Give details of the papers and names of the journals in which it has been published or accepted for publication)
See Annexure B

III. Has the progress been according to original plan of work and towards achieving the objective?
Yes

IV. Please indicate the difficulties, if any, experienced in implementing the project:
No

V. If project has not been completed, please indicate the approximate time by which it is likely to be completed. A summary of the work done for the period (Annual basis) may please be sent to the Commission on a separate sheet

Not Applicable

VI. If the project has been completed, please enclose a summary of the findings of the study. Two bound copies of the final report of work done may also be sent to the Commission.

See Annexure C

VII. Any other information which would help in evaluation of work done on the project. At the completion of the project, the first report should indicate the output, such as (a) Manpower trained (b) Ph. D. awarded (c) Publication of results (d) other impact, if any

See Annexure D

SIGNATURE OF PRINCIPAL

INVESTIGATOR

Dr. Pramod S. Patil
Principal Investigator
U.G.C. major project (2009-2012)
Department of Physics,
Shivaji University,
Kolhapur-416 004

REGISTRAR
Registrar,
Shivaji University, Kolhapur.

Annexure A

Report of the work done

Project Title: **"Layer-by-Layer deposition of multicolored conduction polymer composites for electrochromic smart window application"**	UGC Reference no.: F.No.36-211/2008(SR)

Brief Objective of the report:

Phase-I (First Year):

- To synthesize NiO/Polyaniline (PANI) thin films by a two-step process. A layer of NiO thin films will be electrodeposited on fluorine – doped in oxide coated glass substrates and a layer of PANI will be formed on NiO thin films by a chemical bath deposition.
- To optimize preparative parameter to yield good quality thin films in terms of high coloration efficiency, response time and stability.
- To characterize NiO/polyaniline (PANI) thin films for their structural, optical, morphological and electrochromic properties by using XRD, FT-IR, SEM and cyclic voltammetry respectively.
- To test the electrochromic performance of NiO/polyaniline(PANI) thin films in $LiClO_4$ + propylene carbonate electrolyte.

Phase-II (Second Year):

- To synthesize conducting polymer like polyaniline(PANI), polyethelenedioxythiophene (PEDOT), polypyrrole (PPy) films.
- To synthesize NiO, NiO/conducting polymers prepared by using different surfactant via electrodeposition and chemical bath deposition method.
- To fine tune the process parameter to deposit good quality thin films of complementary conducting composite by layer by layer as well as spin coating techniques.

Phase-III (Third Year):

- To characterize thin films for their electrochromic properties such as, cyclic voltammetry(CV), chronoaperometry (CA), chronopotentiometry (CC) and spectroelectrochemistry.
- Fabrication of electrochromic devices based on these complementary conducting polymers composite and study of their performance.

Annexure B

Electrochromic Device based on NiO/Polypyrrole

X-Ray Diffraction studies

The XRD patterns of NiO, PPy and NiO/PPy films deposited on FTO substrates are presented in Fig 1. Nickel oxide thin film exhibits cubic NiO phase (JCPDS file 4-0835) whereas pure PPy films were found to be amorphous in nature. For the NiO/PPy films, the diffraction peaks of NiO were observed whereas no diffraction peaks of PPy films were found, which indicates, formation of cubic polycrystalline NiO/amorphous PPy samples. The peaks observed at 37° and 43° are of (111) and (200) reflections of cubic NiO. The FTO substrate peaks are denoted by asterisk (*) (JCPDS data file 77-0447).

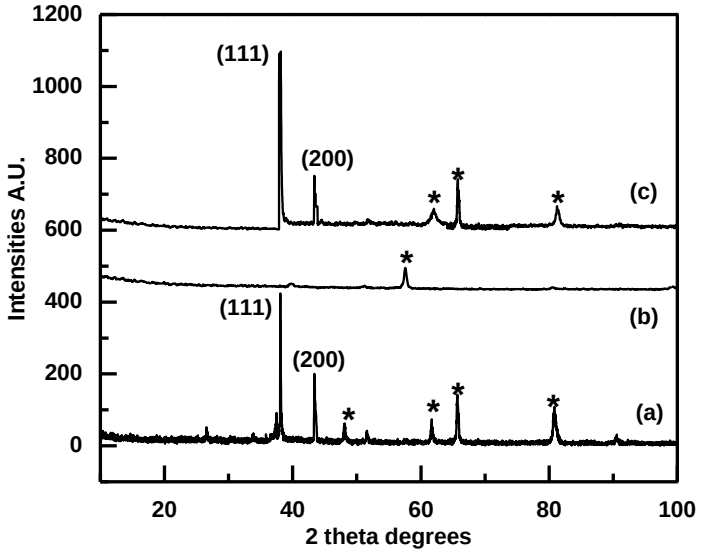

Figure.1. X-ray diffraction patterns for a) NiO, b) PPy and c) NiO/PPy amples where asterisk specifies the peaks of FTO of JCPDS data (77-0447). The standard JCPDS data (4-0835) for NiO is shown as (111) and (200) peaks.

FT-IR spectroscopic studies

The samples in powder form were collected from NiO, PPy and NiO/PPy with the help of doctor blade. The IR spectra of NiO, PPy and NiO/PPy powders in its palletized form with KBr had

been recorded in the range of 400 to 4000 cm^{-1}. Fig.2 shows the FT-IR spectra for NiO, PPy and NiO/PPy samples. The FT-IR spectrum of NiO shows the presence of 6 intensive bands centered at 3438, 1594, 1398, 1114, 668 and 453 cm^{-1} due to OH stretching band of hydrogen bonded water, water bending vibration, in-plane C-H bending mode, incorporation of chloride group and the nickel-oxygen. The PPy spectrum shows the broad strong band at 3420 cm^{-1} corresponds to the absorption of N–H stretching of polypyrrole. The frequency at 2923 cm^{-1} and 2853 cm^{-1} refers to the stretching vibration of C–H bond. The bands at 1565 (2, 5-substituted pyrrole) and 1462 cm^{-1} may be assigned to typical PPy ring vibrations. The bands at 1288, 1041 cm^{-1} may correspond to in-plane vibration of =C–H band. Transmittance peaks 1171 cm^{-1} band was assigned to N-C stretching band and band at 923 cm^{-1} was for the presence of polymerized pyrrole. The IR peak observed at 889 cm^{-1} may be assigned to the out of plane vibration of =C–H indicating polymerization of pyrrole. Whereas in NiO/PPy sample mostly all the stretching vibrations were same as that of NiO and PPy, only a slight shift of IR absorption to lower frequencies in NiO/PPy spectra is observed as compared with NiO and PPy which suggests that an interaction between the polymer and NiO occurs. For NiO films a strong band centered at 453 cm^{-1} corresponds to the stretching vibration of Ni-O. However the shift in NiO stretching band at 490 cm^{-1} was observed in NiO/PPy films. This observed shift in stretching vibration of NiO is due to binding of organic compound to the NiO.

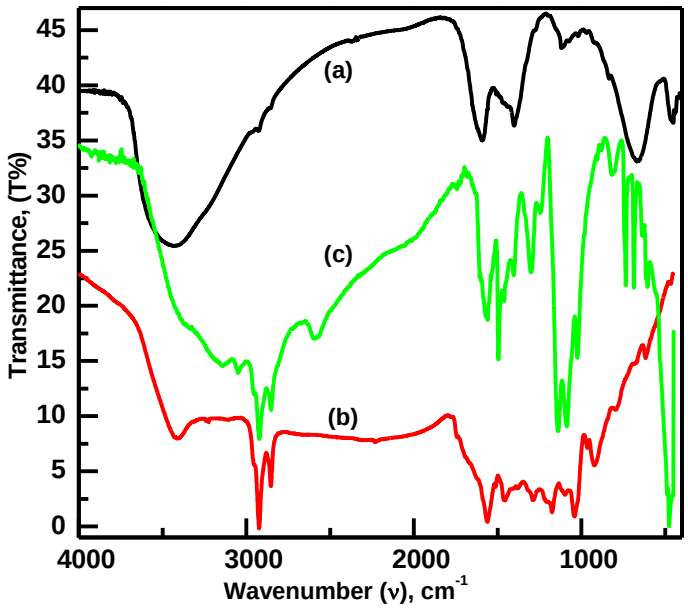

Figure.2. IR transmittance spectra for (a) NiO, (b) PPy and (c) NiO/PPy sample recorded in the wavenumber of 400-4000 cm^{-1}.

The SEM images of NiO, PPy and NiO/PPy films are shown in Fig.3. Surface morphology exhibited by the PPy film deposited onto the amorphous glass substrate is compact, dense and amorphous-like. Nevertheless few grains can be seen. However, when PPy is deposited onto the granular NiO film, large number of faceted grains elongated and rectangular are observed. The underneath NiO grains might have acted as seeds for the growth of these PPy grains. Although randomly grown, their population density is quite uniform.

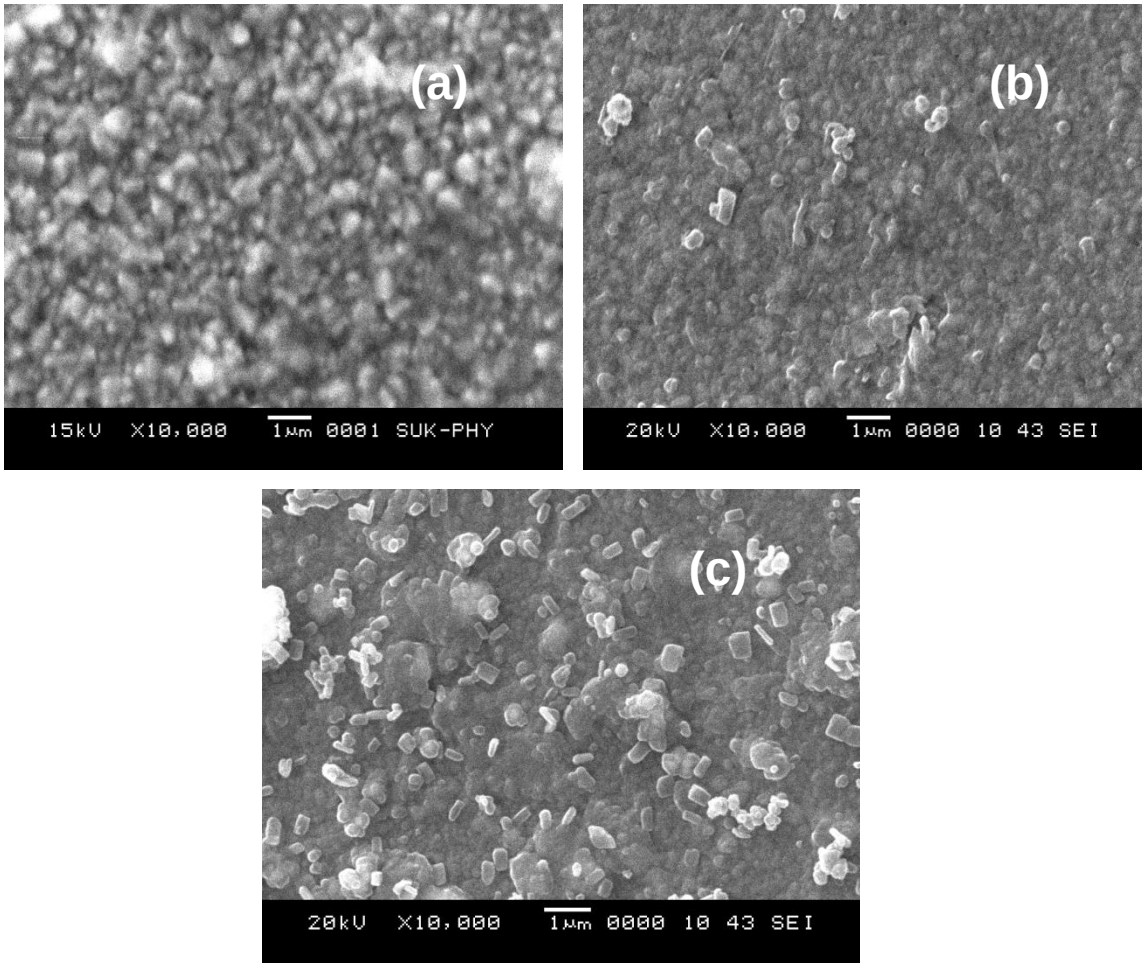

Fig.3(a-c)

Figure.3. Scanning electron microscopy for a) NiO b) PPy and c) NiO/PPy samples deposited onto FTO coated conducting glass substrates. All the films are recorded at X 10000 magnifications.

Electrochromic and electrochemical properties

Fig.4 (a-c) shows the CVs recorded for NiO, PPy and NiO/PPy films in 1M $LiClO_4$ + 1mM PC solution at 20mV/s. The potential scans for NiO thin films (inset of Fig. 4-curve (a)) were started from +2.2 V (vs SCE) reversed at -1.2 V (vs SCE) and terminated at +2.2 V (vs SCE). A well defined cathodic peak at 0.1V (vs SCE) during cathodic scan and anodic peak at 0.9 V (vs SCE) during anodic scans were observed. A simplified reduction scheme representing the gradual optical change that takes place under ion intercalation/deintercalation in EC NiO films is represented in equation (3),

$$NiO_x + yLi^+ + e^- \Leftrightarrow Li_yNiO_x \quad \cdots\cdots\cdots\cdots\cdots\cdots\cdots\cdots\cdots\cdots (3)$$

Transparent Coloured (Brownish gray)

The transition from NiO_x to Li_yNiO_x after intercalation and deintercalation of Li^+ ions causes charge transfer from Ni^{+3} to Ni^{+2}. Due to charge transfer from Ni^{+2} (transparent Fig.4a) to Ni^{+3}, films get colored (brownish gray Fig. 4a).

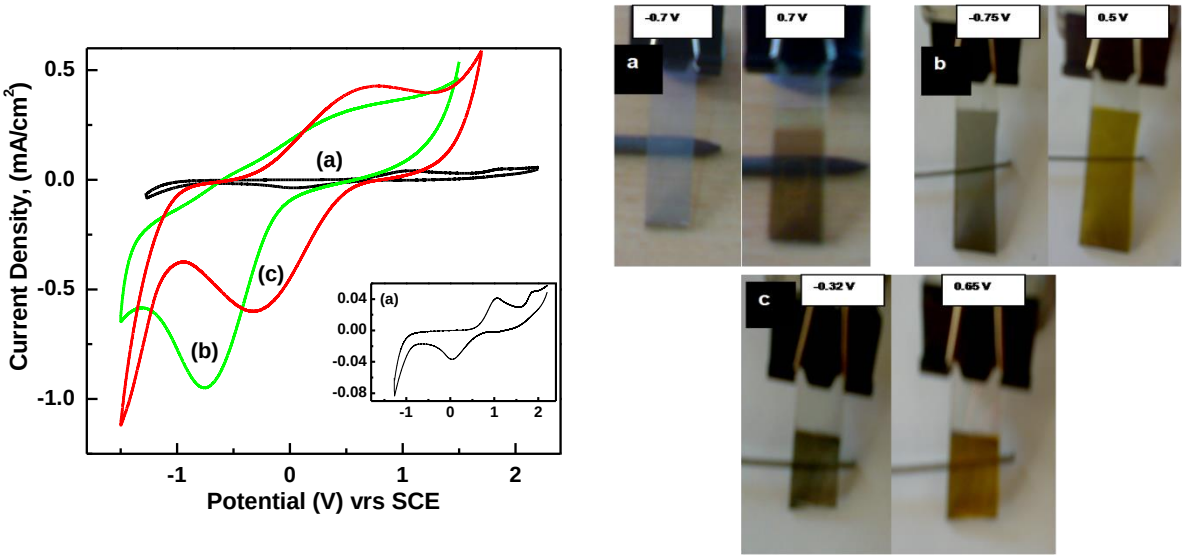

Figure.4. Cyclic voltammogram recorded in 1M $LiClO_4$+PC electrolyte for (a) NiO (also shown in inset), b) PPy and c) NiO/PPy sample. The potential is swept from +2 to -1.2 V (vs SCE) for NiO and +1.5 to -1.5 V (vs SCE) for PPy and NiO/PPy at the scan rate of 20mV/s.

Figure.5. Photographs of a sample (a) NiO (b) PPy (c) NiO/PPy under different applied potentials.

For PPy films, the potential scans were started from +1.5 V (vs SCE) reversed at -1.5 V (vs SCE) and terminated at +1.5 V (vs SCE) (figure 4 curve (b)). A well defined cathodic peak at -0.75 V (vs SCE) during cathodic scan and anodic peak at 0.5V (vs SCE) during anodic scan were observed. Under the above mentioned circumstances, the reaction (4) for PPy films can be described by the scheme:

$$(C_4H_5N)_n + (ny)ClO_4^- \xleftrightarrow{p-doping} [(C_4H_5N^{y+})(ClO_4^-)_y]_n + ny(e^-)$$

Insulating (Orange-yellow) conducting (Black-violet) ---------- (4)

PPy films show electrochromism with color changes from orange-yellow in the reduced state (Fig. 5b) to black-violet in the oxidized state (Fig. 5b). Excluding this it also exhibits an intermediate state changing from yellowish green (-0.8 V vs SCE) to bluish green (-0.62 V vs SCE).

The shape of the CV of NiO/PPy film (Fig. 4 curve (c)) is very similar to the CV of PPy films having cathodic peak at -0.32 V (vs SCE) and anodic peak at +0.65 V (vs SCE) but with less current density, which indicates the presence of NiO. NiO/PPy shows electrochromism with color changes from brown-yellow to black-violet (Fig.5c) which represents that PPy plays leading role in EC of NiO/PPy.

The switching characteristics of the NiO, PPy and NiO/PPy films were studied from in-situ transmittance at 630 nm were performed by switching the samples from an oxidized state to a reduced state by applying alternating square potentials (2.2 and −1.2 V for NiO and 1.5 and −1.5 V for PPy and NiO/PPy). Fig.6 shows the resultant transmittance–time response for all the samples up to first ten cycles. The inset shows the response for one cycle. In these experiments we have chosen the switching times as the times required to switch 95% of the maximum optical contrast at the wavelength of 630 nm. NiO exhibits slower response speed with about 2.75 s for coloration (oxidation) and 1.84 s for bleaching (reduction) kinetics. The response speed is faster in case of PPy samples (1.61 s for coloration and 1.15 s for bleaching). The NiO/PPy samples exhibit much faster response speed (0.601 s for coloration and 0.395 s for bleaching) as compared to pure NiO and pure PPy. The much faster response of NiO/PPy samples stem from the penetration of con-ducting PPy in to NiO pores, which facilitates easy and fast diffusion of ions.

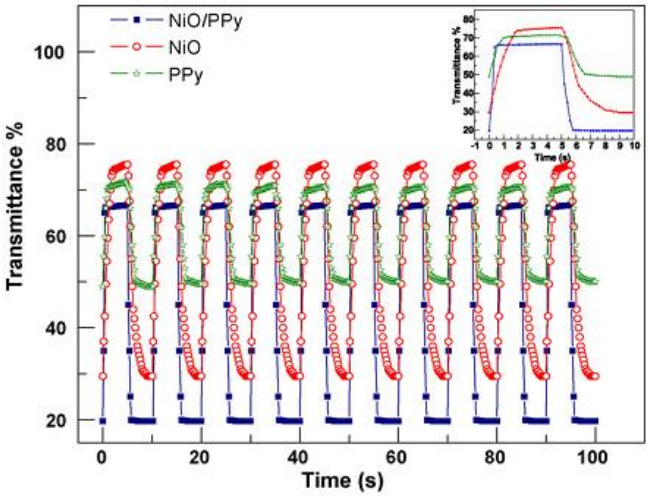

Figure.6. Variation of transmittance for NiO, PPy and NiO/PPy as a function of time for the first ten switching cycles between −1.2 and 2.2 V for NiO and −1.5 and +1.5 V vs SCE for PPy and NiO/PPy in 1 M $LiClO_4$+PC. The inset shows the variation for one complete switching cycle, for all the samples.

The coloration efficiency (CE), an important parameter to probe the potential of the material as an EC material, was calculated at 633 nm by using following relations:

$$CE_{\lambda=630nm} = \frac{(\Delta OD)_{630nm}}{Q_i} \text{ ---------(5)}$$

where (ΔOD) 630nm= Ln (Tb/Tc), and Qi= charge intercalated.

The change in optical density (ΔOD) is found to be 0.72 at 630 nm for the NiO films. The CE of NiO in the reduced and oxidized states is found to be 107cm^2/C. The optical behavior of PPy degrades severely during initial c/b cycling. Fig. 8b shows transmittance change during initial cycling and found that ΔOD changes from 0.7 to 0.45, causing CE to degrade from 181 to 117 cm^2/C, within first 5 c/b cycles. Overall, the PPy sample could remain stable only upto 500 c/b cycles. The optical density of NiO/PPy films found to be 1.43 (fig. 8c) at 630 nm. The CE of NiO/PPy in the reduced and oxidized states is found to be 358 cm^2/C (ΔOD = 1.43, Qi = 4 mC/cm^2). The value was also calculated after 10,000 c/b cycling, which is 299 cm^2/C. Thus when the film of NiO/PPy is formed, the optical density is found to be enhanced appreciably without hampering its electrochemical stability.

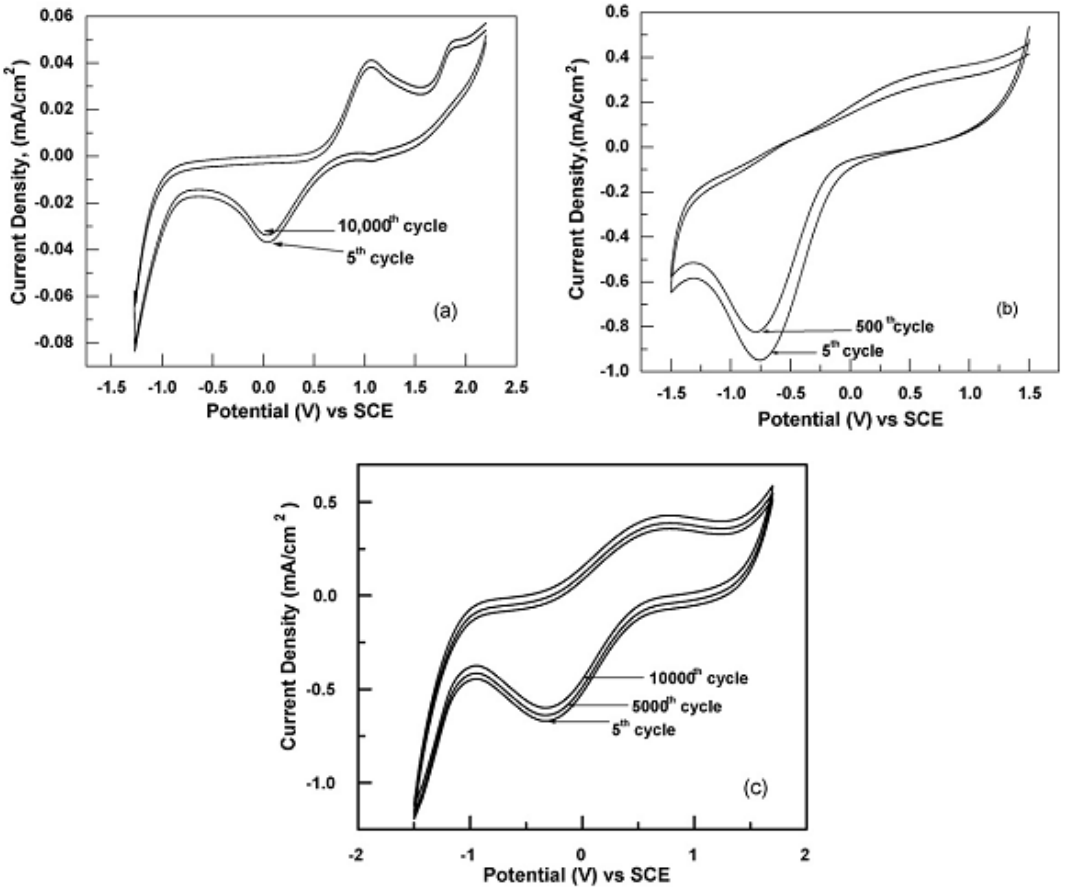

Figure.7. Overlay of CVs for (a) NiO sample after 5th and 10,000th c/b cycle, (b) PPy sample after 5th and 500th c/b cycle and (c) NiO/PPy sample after 5th and 10,000th c/b cycles in 1 M $LiClO_4$ + PC, demonstrating the electrochemical stability of the films at a scan rate of 20 mV/s.

The NiO, PPy and NiO/PPy films were cycled in $LiClO_4$+PC electrolyte for stability testing. Fig.7 (a-c) shows the stability of NiO, PPy and NiO/PPy film. The NiO film is found to be stable about 10^4 or more cycles or more as CV shape and area under the curve remain unchanged (Fig. 7a). As expected, CV degrades severely for PPy films, indicating its poor electrochemical stability (Fig.7b). The anodic peak wanes with increase in the c/b cycles and disappears at 500th cycle and finally the film becomes pale yellow in color and its EC activity is completely lost. However, an excellent electrochemical stability of NiO/PPy can be clearly observed from Fig 7c. The NiO/PPy films are found to be stable for about 10000 c/b cycles. The peak separation (ΔE_p) remains constant. ΔE_p = 1.07 V throughout 10000 cycles. Thus NiO can dramatically elevate the mechanical strength and stability of the PPy films. The advantage of NiO/PPy film is that it enhances EC property of NiO and electrochemical cyclic stability of the PPy, which may be attributed to the chemical bonding between them.

Electrochromic Devices based on NiO/Polyaniline

Structural characterization

The x-ray diffraction (XRD) patterns of the NiO, PANI and NiO/PANI films on FTO substrates are presented in figure 1.The nickel oxide thin film exhibits a cubic NiO phase (JCPDS file 4-835) whereas the pure PANI film has an orthorhombic C6H7N phase (JCPDS file 00-053-1718). For the NiO/PANI films, the diffraction peaks corresponding to both NiO and PANI were observed. The peaks observed at 37◦ and 43◦ are of (111) and (200) reflections of cubic NiO, whereas the peaks at 24◦ and 29◦ are of crystalline PANI structure. However, NiO/PANI has not only two broad peaks centered at 2θ = 37◦ and 43◦ of NiO but also all the sharp peaks of PANI, which proves the existence of PANI in NiO. The peaks at 2θ = 24◦ and 29◦ are observed in NiO/PANI, which are ascribed to the periodicity parallel and perpendicular to the polymer chain of PANI, respectively. It reveals that NiO/PANI and PANI are polycrystalline. The FTO substrate peaks are denoted by an asterisk (*) (JCPDS data file 77-0447).

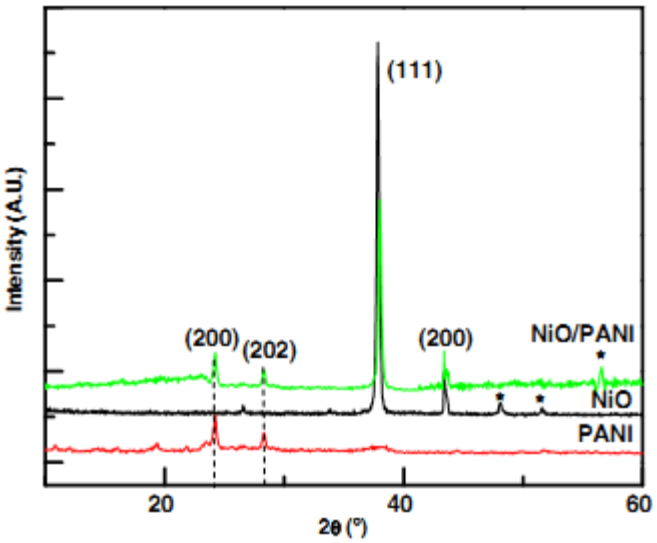

Figure.1. XRD patterns for NiO, PANI and NiO/PANI samples, where asterisk specifies the peaks of FTO of JCPDS data (77-0447).The standard JCPDS data (4-0835) for NiO are shown as (111) and (200) peaks whereas pure PANI film has orthorhombic C_6H_7N phase (JCPDS file 00-053-1718), shown by dashed line.

FT-IR spectroscopic studies

Figure 2 shows the FTIR spectra for the NiO, PANI and NiO/PANI thin films. In the IR spectra of NiO/PANI, the characteristic bands of PANI such as N–H stretching vibration (3218 cm^{-1}), C=C deformation of the quinoid (1571 cm^{-1}), benzenoid ring (1492 cm^{-1}) and out of plane deformation of C–H in the 1,4-disubstituted benzene ring (824 cm^{-1}) were observed. The FTIR spectrum is almost identical to that of PANI but all the bands shifted slightly. The shift in the stretching value and the other interesting feature in the IR spectrum of the NiO/PANI films show the doublet at 1300 and 1247 cm^{-1} which can be attributed to C–N stretching in the bipolaron structure. This reveals an interaction between NiO and PANI. Further, the Ni–O stretching band in the NiO/PANI films is observed at 472 cm^{-1} while for pure NiO it is at 453 cm^{-1}, causing a shift of 19 cm^{-1}. This shift can be attributed to the considerable stretching of Ni–O band due to dative bond formation with nitrogen of PANI. Similar results of coordination bonding between organic–inorganic materials due to the blue shift of N–H stretching vibration were reported by Guo and co-workers.

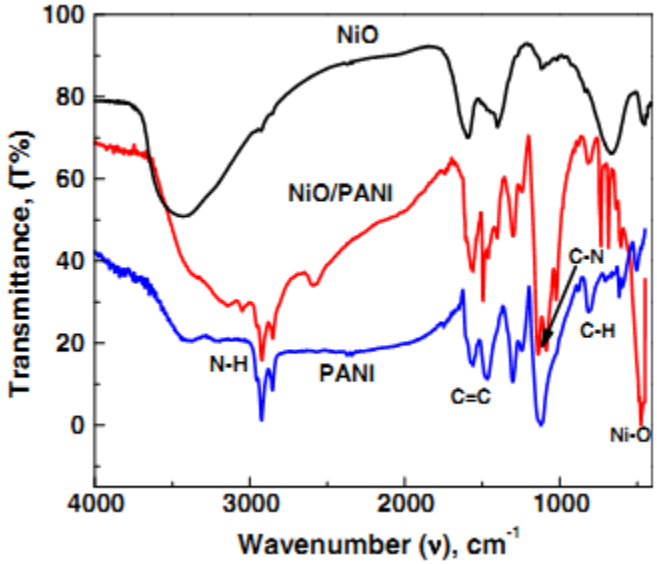

Figure.2. FTIR spectra for NiO, PANI and NiO/PANI samples recorded in the spectral range 400–4000 cm^{-1}.

Morphological study

The SEM images of the NiO, PANI and NiO/PANI films are shown in figure 3. The NiO film reveals a porous granular morphology, whereas the PANI film shows globular morphology. In the

NiO/PANI samples, pores are filled and the surface gets uniformly carpeted with PANI. The porosity of the NiO film is 26% and that of the PANI film is 38%. But when a PANI layer is formed on NiO, the porosity of the NiO/PANI film is found to be decreased to 22%; this may be due to PANI filling up the void spaces of porous NiO. The roughness of the films was measured using a surface profiler and it was found to be about 14 nm, 25 nm and 19 nm for NiO, PANI and NiO/PANI, respectively.

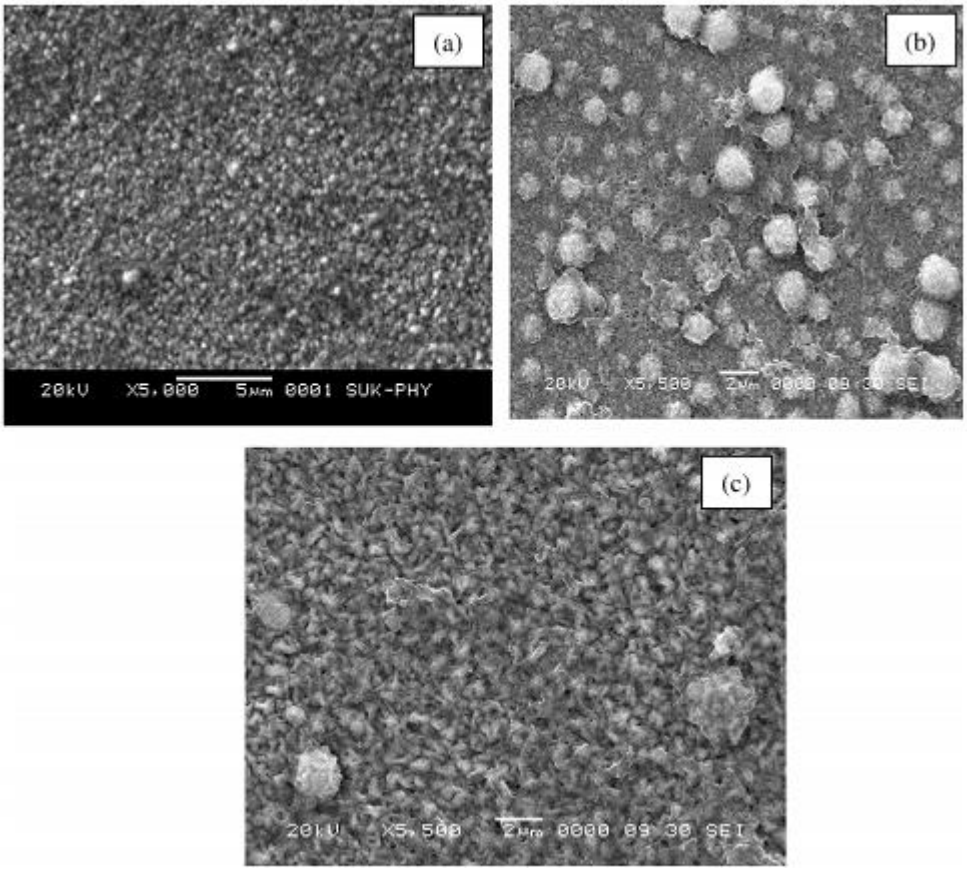

Figure 3. Scanning electron microscopy for (a) NiO (b) PANI and (c) NiO/PANI samples deposited onto FTO coated conducting glass substrates. All the films are recorded at ×5000 magnifications.

Electrochromic and electrochemical properties

The cyclic voltammograms were recorded in the range from −1.5 to 2.2 V (versus SCE) in 1M $LiClO_4$ + PC solution at 20 Mv/s. Figure 4 shows the CVs recorded for the NiO, PANI and NiO/PANI films. The inset depicts the enlarged view of CV for the NiO film. The potential scans were started from −1.5 V (versus SCE) reversed at 2.2 V (versus SCE) and terminated at −1.5 V (versus SCE). Well-defined Cathodic peaks during cathodic scans and anodic peaks during anodic scans

were observed. A simplified reduction scheme that takes place under ion intercalation/deintercalation in electrochromic NiO films is represented by

$$NiO_x + yLi^+ + e^- \leftrightarrow Li_yNiO_x$$

Transparent Coloured (brownish grey)

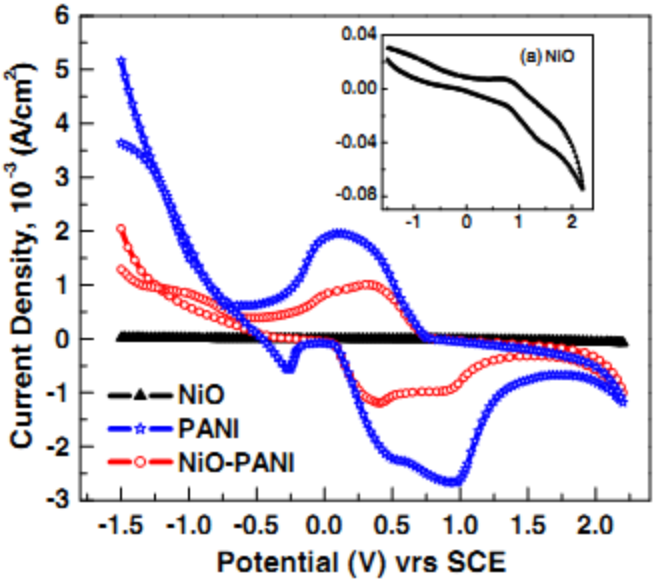

Figure 4. Cyclic voltammogram recorded in 1M $LiClO_4$ +PC electrolyte for NiO (also shown in the inset), PANI and NiO/PANI samples. The potential is swept from +2.2to −1.5 V versus SCE) at the scan rate of 20 mV/s.

The transition from NiO_x to Li_yNiO_x after intercalation and deintercalation of Li^+ ions causes charge transfer from Ni^{3+} to Ni^{2+}. Due to charge transfer from Ni^{2+} (transparent) to Ni3+, the films become colored (brownish grey). The PANI films show electrochromism with colour changes from pale yellow (leucoemeraldine base at −0.7 V versus SCE)–dark green (emeraldine salt at 0.4 V versus SCE)–purple (pernigraniline at 0.8 V versus SCE) in the reduced states to dark blue (nigraniline at 0.5 V versus SCE)– dark green (emeraldine salt at 0.1 V versus SCE)–light green (photomeraldine at −0.3 V versus SCE) in the oxidized states. The shape of the CVs (figure 4) of the NiO/PANI films is very similar to the CV of the PANI films, which shows that PANI plays a lead role in EC of NiO/PANI. It gives the same colouration as mentioned above in PANI but with a higher contrast (contrast for pure PANI = 24% and NiO/PANI = 31%). The colours obtained from the NiO/PANI samples are shown in Figure 5.

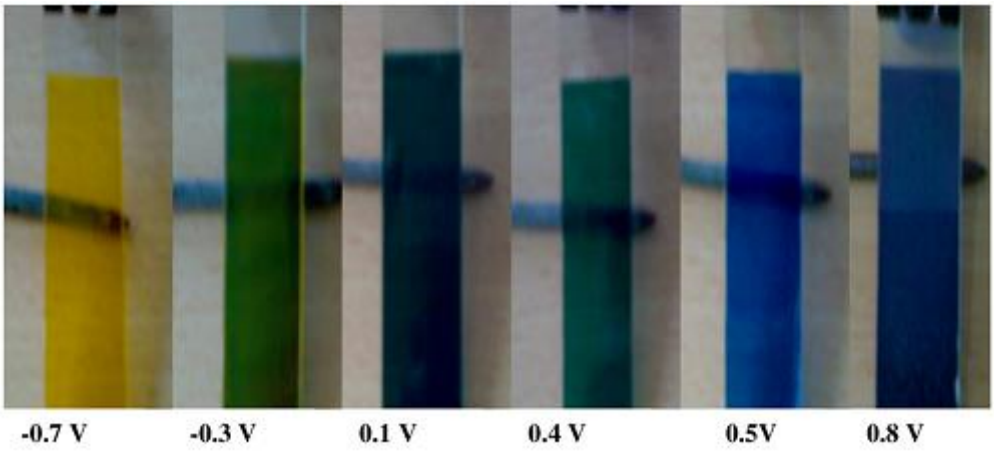

Figure 5. Photographs of a sample NiO/PANI in its coloured state under different applied potentials.

In-Situ Transmittance response time measurement

The switching characteristics of the NiO, PANI and NiO/PANI films were studied using in situ transmittance at 630 nm. The studies were performed by switching the samples from an oxidized state to a reduced state by applying alternating square potentials. Figure 6 shows the resultant transmittance–time response for all the samples, for the first five cycles. The inset shows the response for one cycle. The switching times were measured by considering 95% of the maximum optical contrast at the wavelength of 630 nm. NiO exhibits a slower response speed with about 2.75 s for coloration (oxidation) and 1.84 s for bleaching (reduction) kinetics. The response speed is faster in the case of the PANI samples (300 ms for coloration and 190 ms for bleaching). The NiO/PANI samples exhibit a much faster response speed (60 ms for coloration and 25 ms for bleaching) as compared with pure NiO and pure PANI. The much faster response of NiO/PANI samples stems from the penetration of conducting PANI into the NiO pores, which facilitates easy and fast diffusion of ions. Moreover, for this experiment we have used Li^+ based electrolytes, which can slow the electrochromic response compared with acidic solutions due to the lower electrolyte conductivity. The fastest switching speeds will bring about maximum versatility in applications and it can be used in display devices where switching speeds of milliseconds or less may be required.

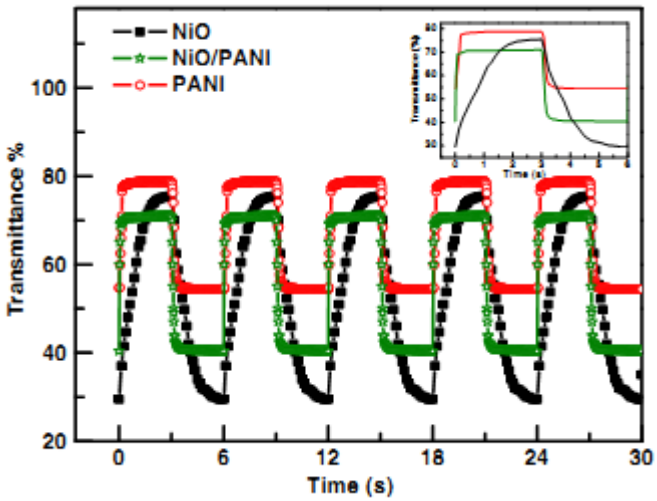

Figure 6. Variation of transmittance for NiO, PANI and NiO/PANI samples at 630 nm as a function of time for the first five switching cycles between −0.7 and 0.7 V for NiO and −0.7 and +0.8 V versus SCE for PANI and NiO/PANI in 1M LiClO4/PC. The inset shows the variation for one complete switching cycle for all the samples.

Figure 7 shows the UV–VIS transmission spectra of the NiO, PANI and NiO/PANI films under different applied potentials. The EC mechanism as well as transmittance of NiO consisting of the transition metal was qualitatively explained by the band structure of the film [51, 52]. The transmittance of the NiO film after c/b at ±0.7 V versus SCE is shown in figure 7(a). The change in optical density (ΔOD) is calculated using

$$\Delta OD_{\lambda=630\,nm} = \ln\left(\frac{T_b}{T_c}\right),$$

where Tb and Tc are the transmittance values for the bleached and coloured states at 630 nm, respectively. ΔOD for the NiO films is found to be 0.72 at 630 nm. The optical density of the PANI films polarized between −0.7 V and +0.8 V versus SCE is also found to be 0.72 figure 7(b)) at 630 nm. The transmittance of NiO/PANI at −0.7 V and +0.8 V versus SCE is shown in figure 7(c). The optical density (ΔOD) of the NiO/PANI films is found to be 1.27 (figure 7(c)) at 630 nm. Thus for the NiO/PANI film, the optical density is found to be enhanced.

The CE, an important parameter to probe the potential of the material as an EC material, was calculated at 630 nm using the following relation:

$$CE_{\lambda=630\,nm} = \frac{(\Delta OD)_{630\,nm}}{Q_i},$$

where (ΔOD)630 nm = ln(Tb/Tc) and Qi = charge intercalated. The CE for the NiO, PANI, NiO/PANI films was found to be 107 cm^2/C, 28cm^2/C, 85cm^2/C, respectively.

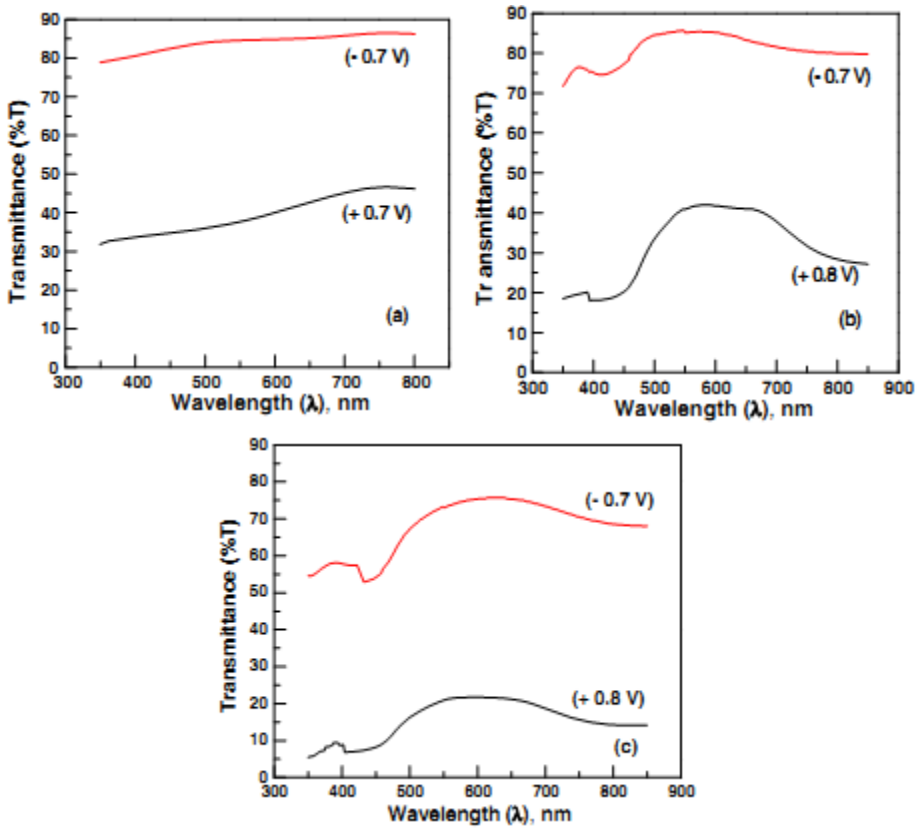

Figure 7. Optical transmittance c/b at different potentials versus SCE in 1M $LiClO_4$ + PC electrolyte for (a) NiO recorded in the wavelength range from 350 to 800 nm (b) PANI and (c) NiO/PANI recorded in the wavelength range from 350 to 850 nm.

The NiO, PANI and NiO/PANI films were cycled in $LiClO_4$ + PC electrolyte for stability testing. Figures 8(a)–(c) show the stability of the NiO, PANI and NiO/PANI films. The NiO film is found to be stable for about 104 cycles or more as the CV shape and area under the curve remain unchanged (figure 8(a)). The stability of our NiO/PANI films is better (104 cycles) as compared with the stability of the porous NiO/PANI films reported by Xia et al (10^3 cycles) [37]. As expected, CV degrades severely for the PANI films, indicating its poor electrochemical stability (figure 8(b)). The anodic peak wanes with increase in the c/b cycles and disappears at the 1000th cycle and

finally the film becomes light green and its EC activity is completely lost. However, an excellent electrochemical stability of NiO/PANI can be clearly observed from figure 8(c).

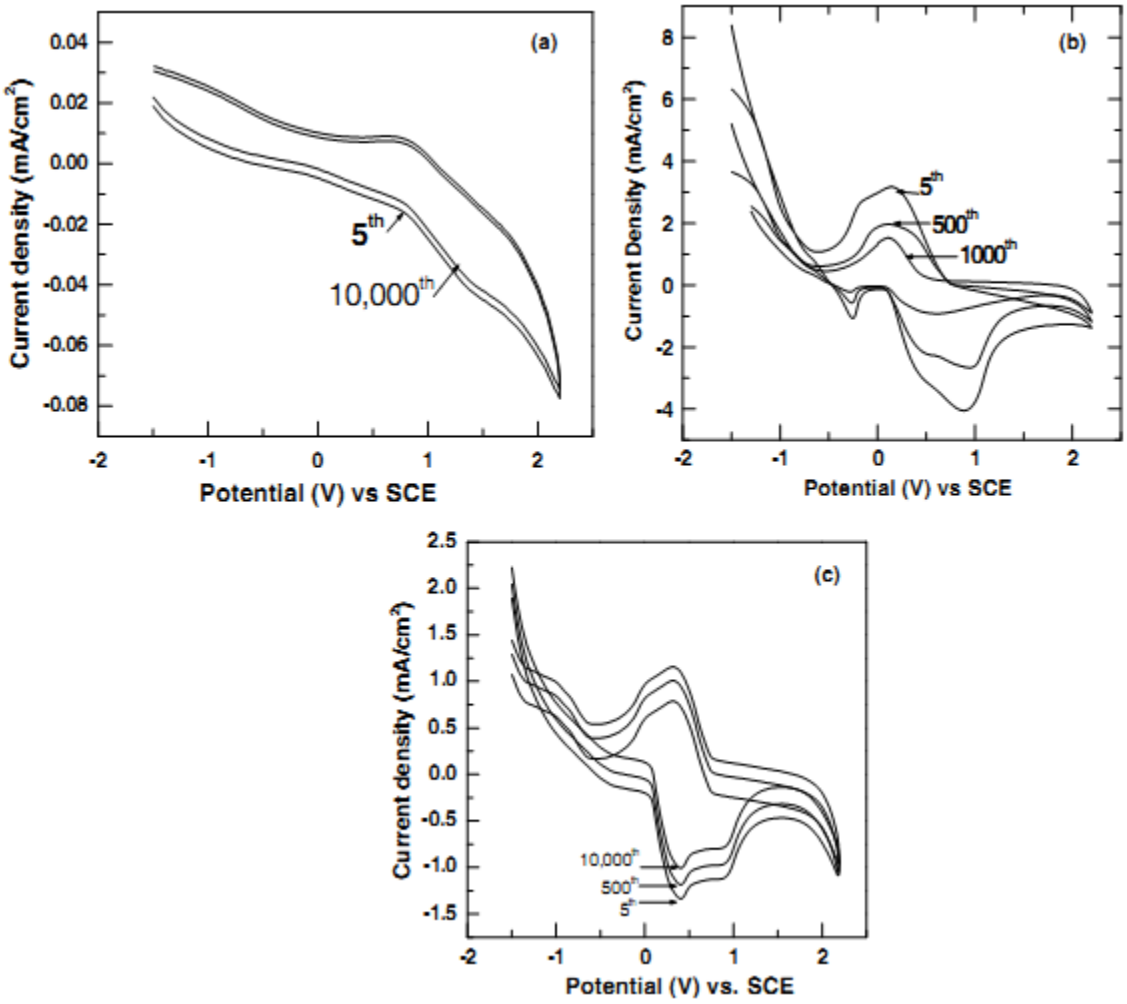

Figure 8. Overlay of cyclic voltammograms for (a) NiO sample after 5th and 10000th c/b cycle (b) PANI sample after 5th, 500th and 1000th c/b cycle and (c) NiO/PANI sample after 5th and 10000th c/b cycles in 1M $LiClO_4$ + PC, demonstrating the electrochemical stability of the films at a scan rate of 20 mV/s.

The NiO/PANI films are found to be stable for about 10 000 c/b cycles. The peak separation (ΔEp) remains constant. ΔEp = 0.44 V throughout the 10 000 cycles. Thus NiO can dramatically elevate the electrochemical stability of the PANI films and PANI can contribute to the faster response time of the device. The advantage of the NiO/PANI film is that it enhances the EC property of NiO and the electrochemical cyclic stability of PANI, which may be attributed to the chemical

bonding between them. However, further characterizations are required to ascertain such bonding between NiO and PANI. This study is underway.

Electrochromic Devices based on WO_3/PEDOT:PSS

Structural and morphological studies:

The thickness of PEDOT:PSS film deposited on the WO_3 film plays a crucial role in the transparency of the system and has to be monitored critically. A very small thickness of PEDOT: PSS film on WO_3 leads to a poor optical contrast with high transparency. If the thickness of PEDOT:PSS layer is increased, it decreases the transparency of the composite film resulting in reduced contrast. A right balance has to be struck between the transparency and thickness in order to get a film incorporating both the advantages without compromising on any feature. Three films were prepared by varying the number of cycles for deposition of PEDOT:PSS from 5 to 15 under optimized conditions. The samples were denoted as WO_3-PP1, WO_3-PP2 and WO_3-PP3 respectively. The thickness of the films was measured using a profilometer. The thickness of WO_3 film forming the base layer was found to be 482nm.This thickness was kept constant for all the three films. The thickness of WO_3-PP1 with 5 layers of PEDOT:PSS on WO_3 was found to be 653nm. WO_3-PP2 had a thickness of 679 nm when 10 layers of PEDOT:PSS were deposited on WO_3while WO_3-PP3 film had a thickness of 822 nm with 15 layers of PEDOT:PSS on WO_3. FE-SEM images were recorded to gather information about the morphology of the bilayered film; Fig.1 shows the FE-SEM images of pure WO_3 and WO_3-PEDOT:PSS films. Fig .1(a) shows the FESEM of R.F. sputtered WO_3 film. The film shows appears to be smooth and featureless with some overgrowth. Fig.1 (b) shows a matrix of WO_3 film dispersed with PEDOT:PSS gel particles. The images show the unique features of both WO_3 and PEDOT:PSS materials. While WO_3 is seen as smooth film with some over-growth, PEDOT:PSS particles are observed as randomly distributed grains making the film a perfectly disordered one. The porous structure is maintained in the composite film which provides easy pathways for ion-intercalation/deintercalation.

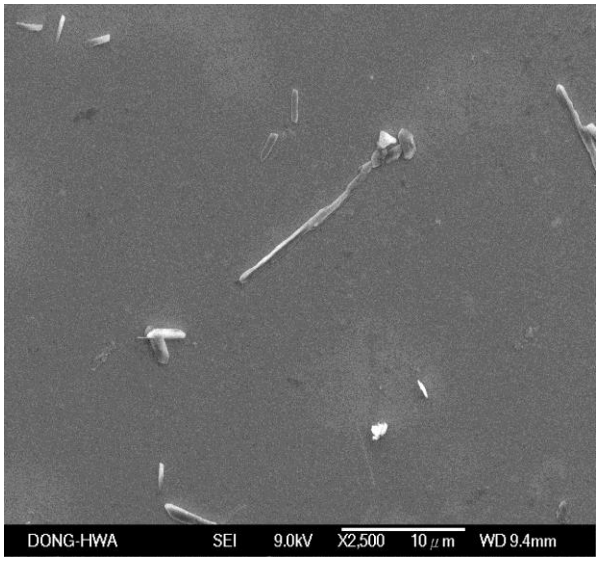

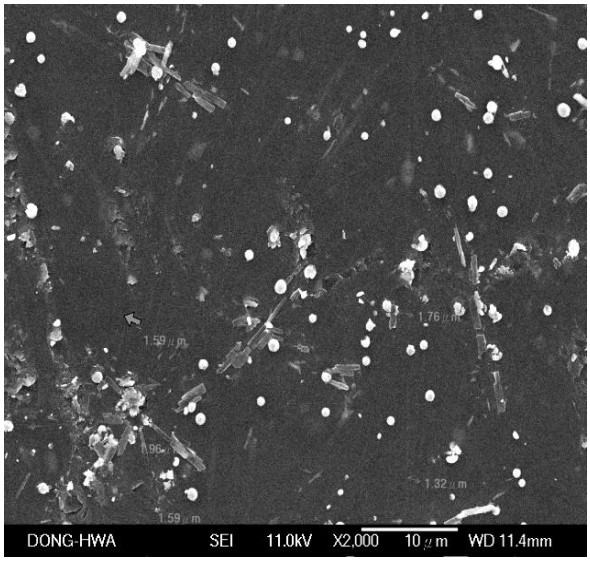

Fig.1(a) Fig.1(b)

Figure.1 FE-SEM images of (a) WO_3 and (b) WO_3-PEDOT:PSS thin films

Electrochromic Properties:

The electrochromic effect, or visible color change in a CP with electrochemical doping, is a direct result of the addition of mid-gap energy levels, producing absorptive transitions in the visible region that invoke an observable color change. In TMO films like WO_3 thin films, optical changes occur due to the formation of H_xWO_3 by the double injection of an electron and a positive ion for charge compensation [31]. The positive ions that can bring about colored or bleached state in WO_3 can be the first group element ions like H^+, Li^+, K^+, Na^+ etc. Electronic transitions between localized states close to the band edge give rise to an absorption process that can be interpreted in terms of intervalence charge transfer.

The electrochemical studies of redox behavior of pure WO_3 and WO_3-PEDOT:PSS thin films were undertaken in an non-aqueous electrolyte with the application of a reversible redox couple at ±1V in a three electrode electrochemical cell with pure WO_3 and hybrid WO_3-PEDOT:PSS layer as working electrode and graphite as the counter electrode. On the application of a reduction potential of -1V, Li^+ ions intercalate into the PEDOT:PSS layer with the charge balancing counter flow of electrons through the external circuit to compensate for the negative charges of the SO_3^- groups on the PSS polyanion reducing PEDOT:PSS layer. The Li^+ ions percolate down to the WO_3 layer with the counter electrons reducing W^{6+} ions to W^{5+} state. These two processes lead to a change in the electron density in the film altering the color of the film from transparent to blue. However, on the

application of oxidation potential of +1V, these Li^+ ions with the counter electrons ,expelled out from the composite film have to migrate to the electrolyte during the reversed oxidation turning the film transparent. The two electrochemical processes [3, 32] that take place simultaneously in the cell at the working electrode can be expressed as:

$$WO_3 + xLi^+ + xe^- \Leftrightarrow Li_xWO_3 \text{----------(1)}$$

$$\left(PEDOT^{x+}PSS^-\right) + xLi^+ + xe^- \Leftrightarrow x\left(PEDOT^0PSS^-Li^+\right) \text{----------(2)}$$

where the left hand side corresponds to the transparent state while the right hand side corresponds to the colored state in both the cases. The cyclic voltammograms (CV) of the pure WO_3 and hybrid bilayered WO_3-PP1, WO_3-PP2 and WO_3-PP3 samples were recorded at a scan rate 40 mV/s are shown in Fig.2 (a-d). Fig.2 (a) shows CV of pure WO_3 sample. The cathodic current density of 2.36 mA/cm^2 was observed for pure WO_3 sample. Fig.2 (b) exhibits a small area under the CV curve for WO_3-PP1 showing feeble charge intercalation and storage capacities. The current density in this case for the reduction process attains a maximum value of 2.6 mA /cm^2. The contribution of PEDOT:PSS film here is very less because its small thickness is unable to play a significant role in the coloration process. Fig.2 (c) shows CV for WO_3-PP2 sample. The CV shows a larger area under the curve and the current density in this case rises to a maximum value of 3.5 mA/cm^2. For the third sample, WO_3-PP3 (Fig.2 (d)), the area under the curve increases with the thickness of the film making available more sites for doping/dedoping taking the maximum current density value for the reduction cycle to 4.2 mA/cm^2.

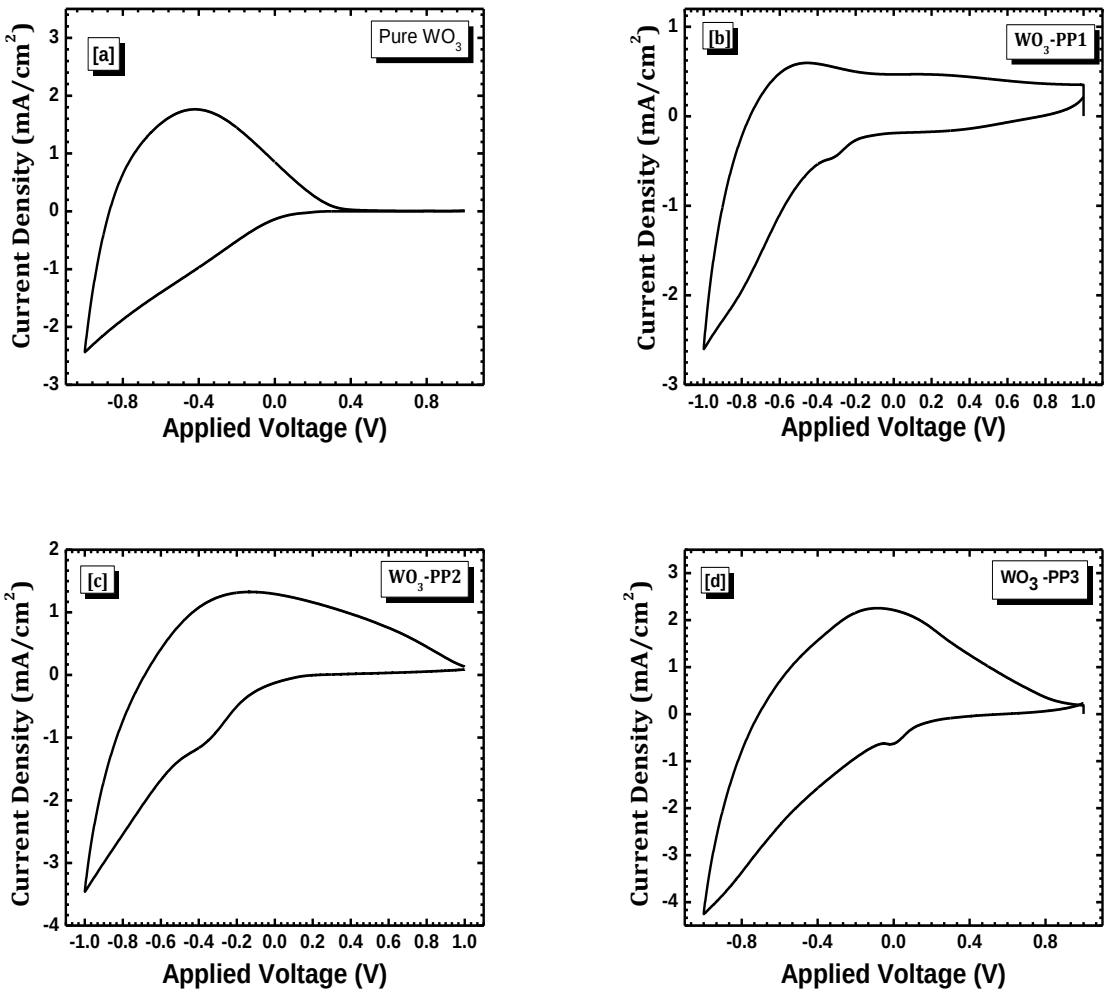

Figure.2 Cyclic voltammograms for (a) pure WO_3 and (b-d) WO_3-PEDOT:PSS thin films in the potential window of ±1 V at 40 mV/s scan rate vs. SCE.

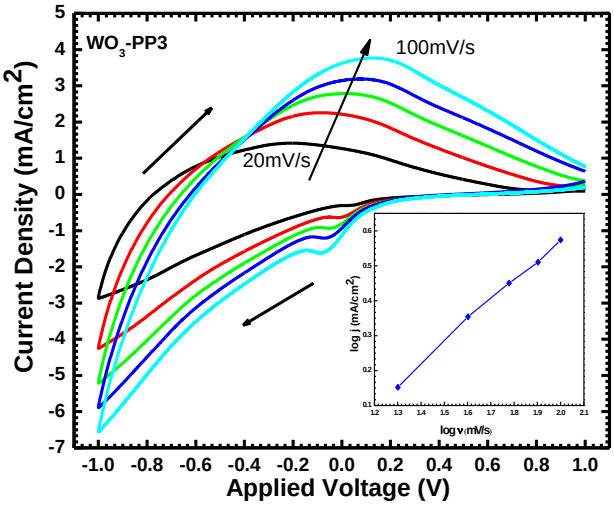

Figure.3 Cyclic voltammograms for sample WO_3-PP3 recorded at different potential sweep rates from 20-100 mV/s vs. SCE. Inset shows the log-log plot of peak current density vs. scan rate.

Apart from FE-SEM, the surface morphology of the bilayered film used as the working electrode has also been studied using the Fractal concept. Fractal dimension (D_f) is a quantitative parameter for analysis of fractal objects using fractal geometry to investigate surface roughness and is one of the most important and useful parameters for analysis of structure of rough surfaces. Stromme et al. suggested the peak-current method to determine the fractal dimension of the electrode surface by using cyclic voltammetry when the recorded cyclic voltammetric current is limited by diffusion of the electroactive species to and away from the electrode surface, the fractal dimension D_f of the reaction site distribution on the surface can be obtained by the following equation:

$$I_{peak} \quad \alpha \quad \nu^{\alpha} \text{ --------(3)}$$

Where, I_{peak} is the peak current; ν is the scan rate and α fractal parameter is related to D_f according to the equation.

$$\alpha = \frac{D_f - 1}{2} \text{ ---------(4)}$$

Since the distribution of the reaction sites provides extensive information about the surface geometry, the fractal dimension of the reaction site distribution may agree with the fractal

dimension of the electrode surface which is completely electrochemically active. The fractal parameter can be obtained easily by plotting the peak current density against sweep rate in a log–log scale using cyclic voltammetry. Typical CV for sample WO_3-PP3 recorded at different potential sweep rates from 20-100 mV/s are shown in Fig.3. The inset shows the log-log plot of peak current density vs. scan rate. The fractal dimensions for all the bilayered WO_3-PEDOT: PSS thin films calculated for the same range of scan rate using equation 4 is listed in Table.1

Optical Transmittance Studies:

The evolution of the electronic band structure during electrochemical can be followed by recording Visible-NIR absorption spectra as a function of applied electrode potential.

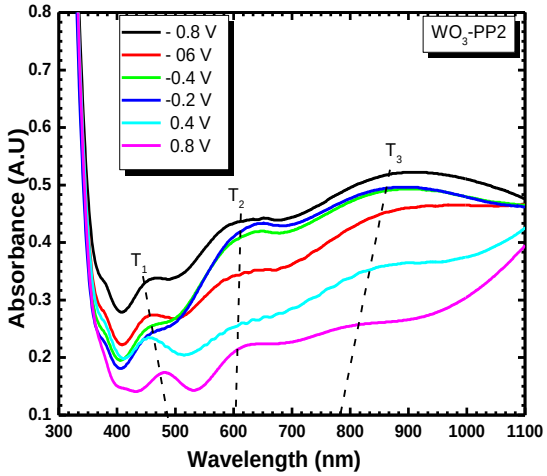

Figure.4 Absorption spectra of WO_3-PP2 at different potentials.

Fig.4 shows the spectroelectrochemical series for the WO_3-PEDOT: PSS bilayer which exhibits a deep blue color in its colored state and a transparent weak blue transmissive state upon oxidation. The spectra show well defined polaron /bipolaron peaks characteristic to the conducting polymers. As the reduction potential is increased gradually from 0.8 to -0.8V, the peak intensity at 485 nm goes on decreasing and shows a hypsochromic shift towards higher energies accompanied with the formation of new bands. An increase in intensity with the broadening of peaks is also observed around 605 nm. The distance between the polaron peaks corresponding to the energy difference increases from 0.03 eV at -0.8V to 0.11 eV at 0.8V. For the entire potential range except at -0.8V, the film shows a broad absorption peak in the NIR at 920 nm with a decrease in the broadness of the peaks as we move towards more positive potentials. This may be because of

electronic transition from the conduction band into newly created bands due to the formation of intermediate energy levels [37].

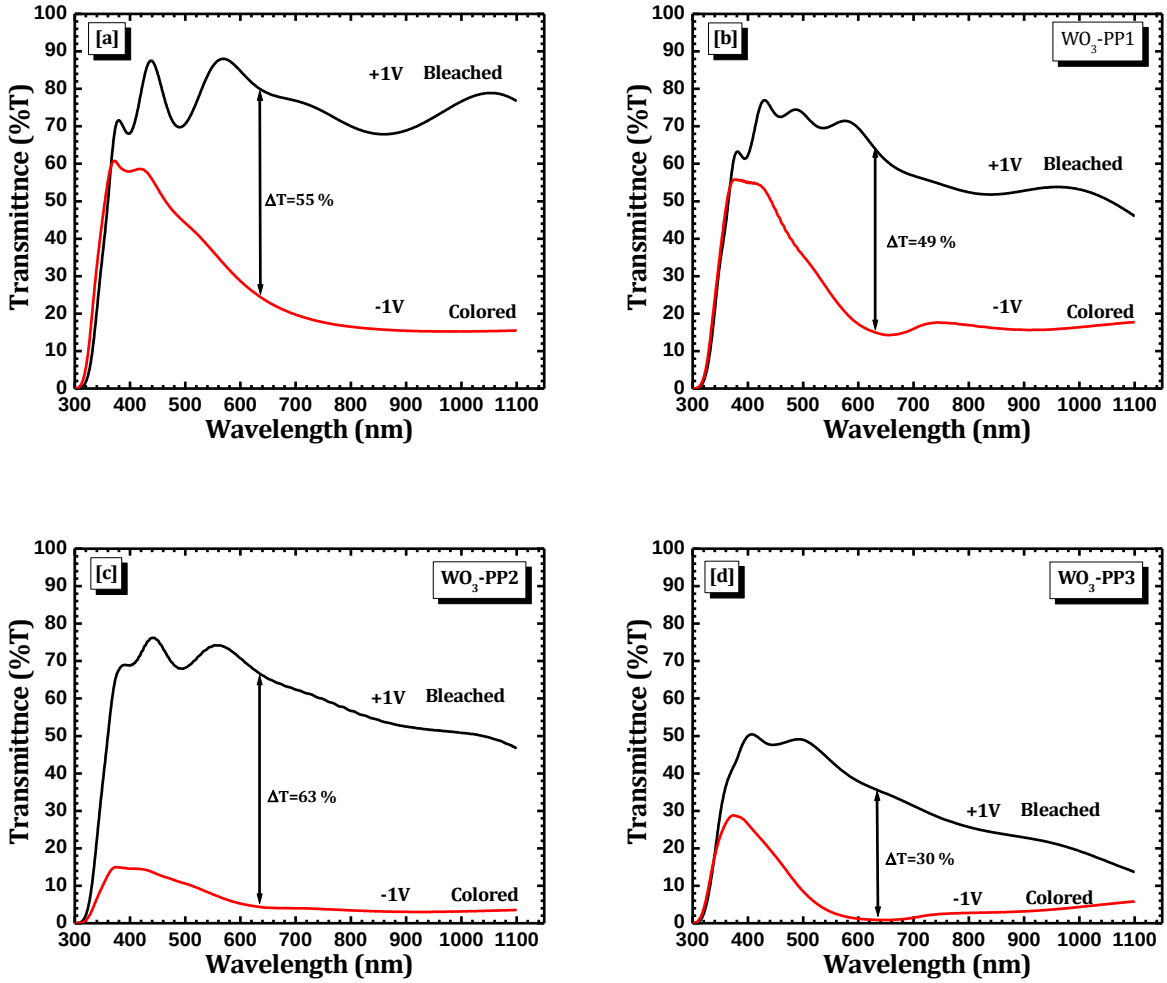

Figure.5 (a-d) Transmittance profile of (a) Pure WO_3 and (b-d) WO_3-PEDOT:PSS (WO_3-PP1, WO_3-PP2, WO_3-PP3) thin films in their colored and bleached states.

Fig.5 shows the transmittance characteristics of the films on the application of the redox potential. The transmittance in the bleached state was found to be 80 % for pure WO_3 (Fig.5 (a)) which reduces to 25 % on the reversal of polarity. The optical modulation for the pure WO_3 was observed to be 55 %. As mentioned before, the thickness of the PEDOT:PSS layer on WO_3 film has to be monitored very judiciously. For sample WO_3-PP1 (Fig.5 (b)), in the oxidized state, the highest transmittance of the sample is 77 % at 430 nm. At 630 nm, the film shows a lesser transparency of 64 %, because of the formation of a polaron. When the negative potential is applied, the

transmittance drops from 64 % to 15% (ΔT=49 %) as the film acquires a deep blue color. Sample WO_3-PP2 (Fig.5 (c)) shows a highest transmittance of 77 % due to interference effects at 440 nm. At 630 nm, the film shows a transmittance of 67 % in the bleached state. On reduction the transmittance in the colored state falls to 4% giving an optical contrast of 63% at 630 nm. When the number of layers of PEDOT:PSS film on WO_3 is increased to 15, for sample WO_3-PP3 (Fig.5 (d)) transmittance in the bleached state decreases to 36 % at 630 nm. The transmittance in the colored state is equal to 1.73%. However, the optical contrast reduces to 30 %. Thus it is seen that both too thin or too thick a layer of PEDOT:PSS on WO_3 film decreases the optical contrast of the device. As optical contrast is an important parameter for ECDs, WO_3-PP2 (thickness=679 nm) was chosen as the optimized sample for all characterizations. The contrat ratio was found by finding the ration of transmittance in the bleached state and colored state at a constant wavelength (λ=630nm).The C.R for the four films are listed in table

The switching characteristics of the WO_3, PEDOT: PSS and hybrid bilayered WO_3-PEDOT:PSS films were studied in-situ transmittance using a laser source (λ=632 nm) and a Si photo detector. The output of the detector was coupled to a storage oscilloscope. Multiple step potential cycling was performed by applying a square wave potential of amplitude ±1V for a time period of 15s. Based on 80% of full response [38], the switching speed from colored-to-bleached state for pure WO_3 is 4.16 s while the bleached to colored switching speed is slightly higher at 8.5 s (Fig.6 (a)). The response time is faster for PEDOT:PSS (1.66 s for coloration and 0.8 s for bleaching) as shown in Fig.6 (b). However, WO_3-PP2 thin film exhibits faster response time as compared to pure WO_3 and it was found the coloration takes place within 5.71 s while the time required for bleaching was 5.59s (Fig.6(c)). For comparison, Fig.6 (d) shows the overlay of the individual layers of WO_3, PEDOT:PSS layers and the bilayered WO_3-PEDOT:PSS device performance for 10 cycles. While the response time of the PEDOT:PSS layer is less, its transmittance change in colored and bleached state is also less whereas for the WO_3 film, both the change in transmittance levels as well as the response time are comparatively quite large. On combining the two layers in the form of bilayered devices, we see that although there is a diminutive decrease in transmittance by 10 % in the bleached state, the response time decreases from 8.33s to 5.71 s making the device switch at a faster rate. The bi-layered WO_3-PEDOT:PSS film therefore combines the good electrochromic contrast of WO_3 with fast switching time of PEDOT:PSS.

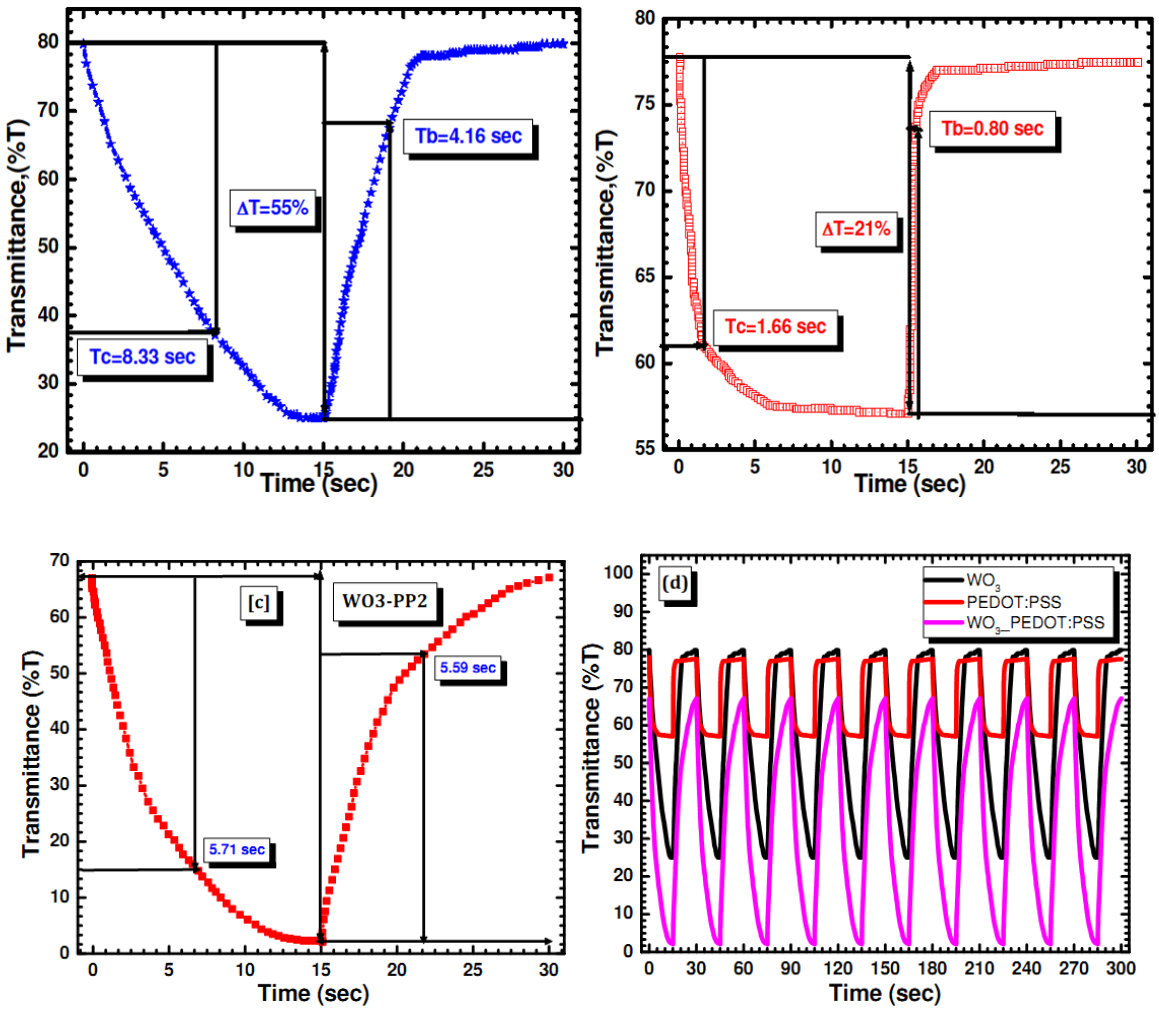

Figure.6 In-situ transmittance time measurement of (a) WO_3 (b) PEDOT:PSS (c) WO_3-PEDOT:PSS (d) Switching characteristic overlay of WO_3, PEDOT:PSS and WO_3-PEDOT:PSS for 10 cycles.

The coloration efficiency (CE) (η) of the bilayered WO_3-PEDOT:PSS film is calculated using the formula given by the equation

$$\eta = \frac{\Delta OD}{Q_i} = \left[\frac{\ln {}^{T_b}/_{T_c}}{Q_i} \right]_{\lambda=630nm} \quad -----(5)$$

where η is the coloration efficiency at a given wavelength λ, T_b is the transmittance in the bleached state, T_c is the transmittance in the colored state and Q_i is the amount of intercalated / deintercalated charge. Table.2 shows the spectroelectrochemical results of the WO_3 and bilayered WO_3-PEDOT:PSS device. The coloration efficiency of the bilayered WO_3-PEDOT:PSS device was found to be 74.60 cm^2/C which is quite high as compared to pure WO_3 (47 cm^2/C) .The enhanced CE

is attributed to a thin layer of PEDOT:PSS on the WO_3 film which reduces number of charges required to color WO_3-PEDOT:PSS thin films and are much lower (22.4 mC/cm^2) than that of pure WO_3 (173 mC/cm^2) thin films. This decrease in charge consumption for coloration may be attributed to the fact that in general conducting polymers require lesser number of charges for coloration. This layer provides an easy pathway for charges to percolate down to the WO_3 layer and bring about an optical change. The bilayered film comprising of dual chromophores exhibits a large CE and higher redox activity i.e higher currents are obtained during the ion intercalation/ deintercalation. The reversibility of the film was found from chronocoulometric measurements using the equation:

$$R = \frac{Q_{di}}{Q_i} \text{-----(6)}$$

Where Q_i is the number of charges intercalated while Q_{di} is the number of ions which deintercalated from the sample .The device exhibits a reversibility of 92 %.

Colorimetry Analysis:

Colorimetric analysis is a well-established characterization technique in the field of organic and inorganic electrochromic films since it allows quantitative measure of the color. It has been used to investigate the properties of electrochromic and light-emitting polymers, blends, and laminates [39] .The colorimetric analysis is based on a set of color coordinates, such as the CIE 1931 Yxy color space (Fig7a).

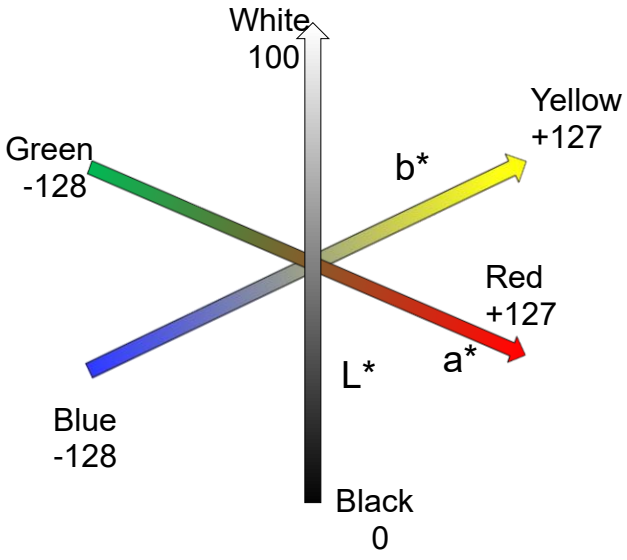

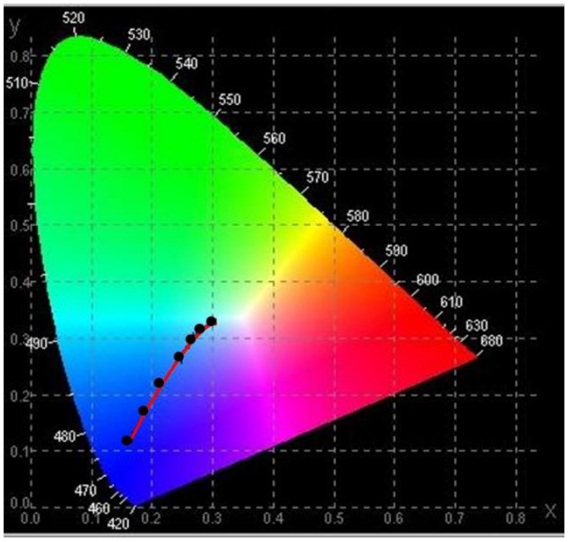

Fig 7(a) Fig 7(b)

Figure.7(a) CIE L*a*b* system **(b)** CIE 1931 Yxy Chromaticity diagram for WO_3-PEDOT:PSS bilayered film for a 2° observer and D-65 illuminant.

In this color space, Y corresponds to the brightness or luminance of a color, whereas the xy coordinate of a color defines its hue and saturation [40]. Both luminance and x-y chromaticity diagrams provide valuable information for understanding changes in the devices color and/or brightness. For example, the potential dependence of the relative luminance offers a perspective on the transmissivity of a material as it relates the human eye perception of transmittance over the entire visible spectrum as a function of potential on a single curve. The chromic contrast of the novel bilayered ECD was found by finding the difference in the luminance value between the light state and the dark state as defined by

$$\Delta L^* = L^*_{Bleached} - L^*_{Colored} \text{ ------(7)}$$

where $L^*_{Bleached}$ and $L^*_{Colored}$ are the luminosity in the bleached and colored states respectively using CIE co-ordinates for a 2° observer and D-65 illuminant

In the bleached state, the bilayered device shows a L* value of 88.05. A value of L* close to 90 indicates a highly transparent nature of the film. The value of ***a**** is -1.37 and ***b**** is equal to 3.18 in the transparent state**.** On the application of polarizing voltage of -1V, the L* value decreases to 56.95. The value of a* changes to -0.42 with a corresponding increase in b* value to -28.89. The higher value of b* shows a shift towards the blue color. The overall luminance change, that is, in essence the chromic contrast is equal to 31%. The change in color of the device on the application of different potentials is plotted on the chromaticity diagram. Fig.(7b) shows the hue and saturation x-y track as the applied potential is changed from +1 to -1V, which corresponds to the reduction cycle of the bilayered device. The curve is found to be almost linear staring from (0.32, 0.34) in the transparent state to (0.18, 0.12) in the colored state**.**

Annexure C

Summary of the findings of the study:

The present research work is devoted for the study of conducting polymer composite thin films, which applicable in the electrochromism technology as well as in semiconducting thin film physics. Therefore we have undertaken structural, morphological, optical and electrochemical studies on these films that have helped to arrive at following conclusions:

- NiO thin films of different thicknesses with change in deposition time have been successfully deposited by a simple and cost effective chemical bath deposition method. It is observed that the film thickness as well as the choice of suitable electrolyte plays a crucial role for enhancing the electrochromic properties. The electrochromic CE of the films is found to be two times more in $LiClO^4$-PC than that observed in more often used KOH electrolyte with increase in film thickness. The nanoporous interconnected nanopetal network with well-defined 3D nano envelopes facilitates the control over the surface area and porosity/open structure, affecting the ion insertion kinetics (ion diffusion length and time, ionic mobility, etc.) leading to enhanced EC performance. Finally, it is concluded that the electrochromic properties of the NiO films can be tailored merely by controlling the film thickness and choice of suitable electrolyte which will be potentially useful for designing complementary EC devices.

- An electrochromic NiO/PANI film was assembled with a configuration of FTO/NiO/PANI and characterized for its electrochromic and optical performance in $LiClO_4$+PC. XRD indicates that the film composed of NiO and PANI is in the crystalline form, in which nickel oxide is in the form of NiO. FTIR reveals a dative bonding between nitrogen of PANI and nickel of NiO. Scanning electron micrographs reveal a compact granular morphology of NiO which gets uniformly carpeted with PANI leading to a matty morphology. The CE of the NiO/PANI film was observed to be 85 $cm^2\ C^{-1}$. These results were suitable to operate the film with perceptible colour changes from yellow to green in the potential range from −0.7to+0.8 V. The

sample changes colours from yellow to light green with intermediate steps of green, violet, blue and dark green. The response time of the film for the colouring and bleaching process was found to be 60 ms and 25 ms, respectively. The stability of the NiO/PANI film is about 10 000th c/b cycles. The NiO/PANI film is that which enhances the EC property of NiO and the electrochemical cyclic stability of PANI.

- An electrochromic NiO/PPy film was assembled with a configuration of FTO/NiO/PPy and characterized for its electrochromic and optical performance in LiClO4+PC. XRD and FTIR indicate that the film composed of NiO in cubic crystalline form and PPy is amorphous in nature. Scanning electron micrographs reveals a large number of faceted rectangular grains. The CE of the NiO/PPy film was observed to be 358 cm^2/C. These results were suitable to operate the device with perceptible color changes from brown–yellow in the reduced state to black–violet in the oxidized state in the potential range from−1.5 to +1.5V (vs SCE). The response time of the film for coloring and bleaching process were found to be 0.601 and 0.395s, respectively. This indicates the faster insertion and deinsertion kinetics. The stability of NiO/PPy film is about 10^4 c/b cycles. The NiO/PPy film thus exhibits enhanced EC property owing to the chemical bonding between them.

- A novel bilayered device has been synthesized by spin deposition of PEDOT:PSS layers on R. F. sputtered WO_3 films. FE-SEM images show that amorphous domains of PEDOT:PSS resides along with the WO_3 host in the bilayered film. Using the fractal approach,fractal dimensions have been calculated. The WO_3-PEDOT:PSS film shows a faster switching response with 5.71 and 5.59 s for coloring and bleaching respectively as seen from in-situ characterizations. The change in values of xy co-ordinates have been plotted on a chromaticity diagram .The curve on the chromaticity diagram is seen to follow a linear path as the color transition takes place from transparent to blue and vice versa. The film, being a dual electrochrome, exhibits a large CE of 74.6 cm^2/C and a higher redox activity attributed to a thin layer of PEDOT:PSS on the WO_3 thin film. An important advantage of using PEDOT:PSS is the possibility of ease of application with technically established

coating techniques, such as casting, spray,ink-jet apart from spin coating for large-area coating of WO_3 films. Thus with a small sacrifice of transmittance in the clear state, this bilayered device which is less power intensive with a higher CE, an economically viable product can be realized.